



Continuous twin screw granulation: Impact of microcrystalline cellulose batch-to-batch variability during granulation and drying – A QbD approach

Christoph Portier^a, Tamas Vigh^b, Giustino Di Pretoro^b, Jan Leys^b, Didier Klingeleers^b, Thomas De Beer^c, Chris Vervaet^a, Valérie Vanhoorne^{a,*}

^a Laboratory of Pharmaceutical Technology, Department of Pharmaceutics, Ghent University, Ottergemsesteenweg 460, B-9000 Ghent, Belgium

^b Drug Product Development, Janssen Research and Development, Turnhoutseweg 30, B-2340 Beerse, Belgium

^c Laboratory of Pharmaceutical Process Analytical Technology, Department of Pharmaceutical Analysis, Ghent University, Ottergemsesteenweg 460, B-9000 Ghent, Belgium

ARTICLE INFO

Editor: Juergen Siepmann

Keywords:

Continuous manufacturing
Twin screw granulation
Wet granulation
Formulation development
Batch-to-batch variability
Quality-by-Design
Design of experiments

ABSTRACT

Despite significant advances in the research domain of continuous twin screw granulation, limited information is currently available on the impact of raw material properties, especially considering batch-to-batch variability. The importance of raw material variability and subsequent mitigation of the impact of this variability on the manufacturing process and drug product was recently stressed in the Draft Guidance for Industry on Quality Considerations for Continuous Manufacturing by the U.S. Food and Drug Administration (FDA). Therefore, this study assessed the impact of microcrystalline cellulose (MCC) batch-to-batch variability and process settings in a continuous twin screw wet granulation and semi-continuous drying line. Based on extensive raw material characterization and subsequent principal component analysis, raw material variability was quantitatively introduced in the design of experiments approach by means of t1 and t2 scores. L/S ratio had a larger effect on critical granule attributes and processability than screw speed and drying time. A large impact of the t1 and t2 scores was found, indicating the importance of raw material attributes. For the studied formulation, it was concluded that MCC batches with a low water binding capacity, low moisture content and high bulk density generated granules with the most desirable quality attributes. Additionally, an innovative and quantitative approach towards mitigating batch-to-batch variability of raw materials was proposed, which is also applicable for additional excipients and APIs.

1. Introduction

In the last decade, significant progress has been made in the field of continuous pharmaceutical manufacturing. Supported by a progressive mindset of regulatory agencies, several global pharmaceutical companies such as Janssen, Vertex, Lilly and Pfizer have achieved market approval for drug products manufactured through continuous manufacturing techniques, such as direct compression or twin screw wet granulation (Portier et al., 2020c; U.S. Food and Drug Administration, 2018; Yu, 2016). As these techniques are associated with shorter supply chain times, patients can rely on faster access to innovative and high

quality drug products. Additionally, these production pathways offer clear economic advantages over batch manufacturing such as a lack of scale-up, lower floor space requirement, design flexibility and real time release testing (Byrn et al., 2015; Ito and Kleinebudde, 2019; Thompson, 2015; Vervaet and Remon, 2005).

The advances in the field of twin screw wet granulation have been strongly supported by academic research closely related to drug product registration and quality by design. A large subsection of this research is focused on process understanding and optimization through experimental designs (Djuric and Kleinebudde, 2008; Meier et al., 2017; Portier et al., 2020c, 2020b; Thompson and Sun, 2010; Vercruyssen et al.,

Abbreviations: API, Active Pharmaceutical Ingredient; BET, Brunauer Emmett and Teller; Com, Commercial batch; DoE, Design of Experiments; Dx (d10, d50, d90), Size in microns at which x volume% of the particles is smaller than dx; HR, Hausner Ratio; L/D, Length-to-diameter; LOD, Loss on drying; L/S, Liquid to solid; MCC, Microcrystalline Cellulose; PCA, Principle Component Analysis; PSD, Particle size distribution; rpm, Revolutions Per Minute; RTD, Residence Time Distribution; SCE, Size Control Element; SSA, Specific Surface Area; QbD, Quality-by-Design; WBC, Water Binding Capacity.

* Corresponding author.

E-mail address: Valerie.Vanhoorne@UGent.be (V. Vanhoorne).

<https://doi.org/10.1016/j.ijpx.2021.100077>

Received 17 March 2021; Accepted 18 March 2021

Available online 19 March 2021

2590-1567/© 2021 The Authors.

Published by Elsevier B.V. This is an open access article under the CC BY-NC-ND license

(<http://creativecommons.org/licenses/by-nc-nd/4.0/>).

2015, 2012) and modeling (Liu et al., 2019; Shirazian et al., 2019). Through the integration of process analytical technology (PAT) and appropriate control strategies, the quality of drug products and intermediates can be continuously monitored and regulated, hence avoiding non-conforming material (Harting and Kleinebudde, 2018; Madarász et al., 2018; Pauli et al., 2019; Verstraeten et al., 2018).

Despite recent advances, there is still a large knowledge gap on the impact of material attributes as most studies are limited to a single formulation in which component characteristics are not varied (Thompson, 2015). Although some studies assessed the impact of different material grades (El Hagrasy et al., 2013; Fonteyne et al., 2014; Vanhoorne et al., 2016a) in twin screw wet granulation, limited information is available on batch-to-batch variability of raw materials and its significance in twin screw wet granulation lines. Fonteyne et al. described the effect of differences in water binding capacity (WBC) of microcrystalline cellulose (MCC), affecting granule size distribution. These differences were attributed to a different degree of crystallinity (Fonteyne et al., 2015). Stauffer et al. were the first to report on the impact of active pharmaceutical ingredient (API) batch-to-batch variability induced by different synthetic routes and by varying the crystallization and drying equipment. In these studies, the impact of API batch-to-batch variability on the different unit operations of a continuous tableting line including twin screw granulation was reported (Stauffer et al., 2019a, 2019b).

Previous work from our group identified lactose/microcrystalline cellulose in a 1:1 ratio as a suitable and robust filler combination for granulating APIs with different properties at varying drug loads (Portier et al., 2020b, 2020d, 2020a). However, MCC was identified as a potential source of batch-to-batch variability due to its natural origin (wood pulp) and high number of processing steps (Fonteyne et al., 2015; Portier et al., 2020a). As a previous study on MCC batch-to-batch variability was restricted to a single unit operation (twin screw wet granulation) in continuous manufacturing (Fonteyne et al., 2015), this study aims to further elucidate the potential relevance of MCC batch-to-batch variability in a continuous line comprising a twin screw granulator and fluid bed dryer. Furthermore, a quantitative strategy will be applied for mitigating batch-to-batch variability.

2. Materials and methods

2.1. Materials

α -Lactose monohydrate (Pharmatose 200 M) and 12 batches (6 commercial (Com) and 6 Quality-by-Design (QbD) batches) of MCC (Avicel PH 101) were kindly donated by DFE Pharma (Goch, Germany) and DuPont (Wilmington, DE, USA), respectively. These fillers were used in a 1:1 w/w ratio. MCC QbD batches were selectively prepared by DuPont to induce larger variability than during standard commercial manufacturing. Variability was induced by combining specific pulp mixes or by using pulp mixes with particle size properties outside the standard manufacturing limits. Metformin hydrochloride was provided by Janssen and was added as low-dosed API in a 5 wt% concentration. HPMC E15 LV was selected as dry binder (5 wt%) and was supplied by Dow (Midland, MI, USA).

2.2. MCC characterization

2.2.1. Loss on drying

The moisture content of the MCC batches was analyzed in triplicate using a Mettler Toledo LP 16 moisture analyzer (Mettler Toledo, Zaventem, Belgium). For each analysis, 1 g of MCC was heated to 105 °C until a stable mass was registered for 30 s. Loss on drying (LOD) values were defined as the percentual loss in mass, relative to the initial mass.

2.2.2. Particle size distribution

Particle size distribution (PSD) was determined in triplicate through

laser diffraction. Powder was fed at a jet pressure of 2 bar and feed rate of 3 g with the MS64 dry powder feeder unit of the Malvern Mastersizer S equipped with a 300F lens (active beam length 10 mm). Subsequently, d10, d50 and d90 were derived from the calculated volume distribution (polydisperse model). Dx was defined as the size in microns at which x volume% of the particles is smaller than dx. To indicate the PSD width, span ratio was calculated as the ratio between (d90-d10) and d50.

2.2.3. Bulk and tapped density

Bulk density was evaluated ($n = 3$) using a standardized tapping device (Pharma Test, Hainburg, Germany). 100 g of material (m) was loaded into a glass cylinder of 250 ml. From the ratio between the mass (m) and the initial volume (V_0), bulk density (ρ_B) was calculated. Subsequently, the glass cylinder was positioned on the tapping device (Pharma Test, Hainburg, Germany) and the volume was registered after 750 and 1250 taps. If the volume difference exceeded 2 ml, 500 additional taps were performed to determine the tapped volume (V_t), from which the tapped density (ρ_T) was derived as the ratio between m and V_t .

2.2.4. Specific surface area

MCC samples (± 1 g) were initially degassed at 60 °C for 24 h using the vacuum mode of the VacPrep (Micromeritics, Norcross, USA) and subsequently purged with nitrogen for one hour. Nitrogen adsorption measurements were performed at 77 K using a 7 point method (TriStar II, Micromeritics). The specific surface area (SSA) of the MCC samples was determined using the Brunauer Emmett and Teller (BET) adsorption isotherm.

2.2.5. Hygroscopicity

Hygroscopicity was determined using a desiccator with a saturated $MgCl_2$ solution, ensuring a relative humidity of 33%. Samples of 2 g were left to equilibrate for a period of 96 h at 20 °C. To mimic the behavior of the samples in normal manufacturing conditions, these were not pretreated before equilibration. The reported hygroscopicity was defined as the moisture uptake (%), relative to the initial sample mass.

2.2.6. Water binding capacity

Water binding capacity (WBC) of the MCC samples was assessed in triplicate. A sample of 5 g was suspended in 20 ml of demineralized water. The suspension was subsequently centrifuged for 20 min at 5000 g. After decantation of the supernatant, the mass of the MCC pellet was determined. The WBC was defined as the percentual water uptake, relative to the initial MCC mass.

2.2.7. Contact angle

An OCA 50 AF contact angle meter (DataPhysics Instruments, Filderstadt, Germany) was used to perform sessile drop contact angle measurements ($n = 9$). Three microscopy slides, each suitable for evaluating three drops, were prepared for each sample. Each slide was provided with a layer of double-sided tape and subsequently transferred on top of a powder bed consisting of MCC. The excess material was removed with compressed air and 2 μ l drops of demineralized water were dispensed on the slide. Average contact angles after 1, 10 and 45 s were derived from the average of the left and right contact angles, which were calculated using the SCA 20 software (version 5.0.24).

2.3. Principal component analysis

Due to limited average differences and relatively high standard deviations, no discrimination between batches could be made for properties derived from specific surface area and contact angle measurements. Therefore, SSA and contact angle data were not included in the final dataset. SSA values were situated near the lower detection limit of the equipment. For contact angle measurements, this was attributed to the rather low contact angle (45–50°) of MCC, generating relatively high standard deviations. Potentially, lower standard deviations could be

achieved with other wettability characterization techniques, such as the Washburn capillary rise method, which is more suitable for low contact angle measurements.

All remaining raw material characteristics were centered, scaled to unit variance and related material properties were grouped (Table 1) to assure a block unit variance of 1. This was done by applying a block weight of $\frac{1}{\sqrt{n}}$ for each block, with n being the number of variables in a respective block. No transformations were applied to the dataset, as no variables had a skewed distribution. Subsequently, a PCA model with three principal components was developed using Simca (v16.0.2.10561, Sartorius Stedim Biotech, Malmö, Sweden). This model captured 92% of the dataset variability (R^2X , goodness of fit) and was able to predict 70% of the total variation in the dataset (Q^2).

2.4. Preparation of granules

Due to its cohesive nature, metformin hydrochloride was first milled using a Quadro U5 Comil equipped with a 1397 μm round holed screen and a round bar impeller operating at 3000 rpm (Quadro, Waterloo, Canada). Raw materials (5% metformin.HCl, 45% lactose, 45% MCC and 5% HPMC) were blended in a tumbling blender (Inversina Bioengineering, Wald, Switzerland) during 15 min at a rotational speed of 25 rpm. Subsequently, the blend was gravimetrically fed using a KT20 twin screw feeder (K-Tron, Niederlenz, Switzerland) towards the temperature-controlled granulator (ConsigmaTM-25, GEA, Düsseldorf, Germany) barrel ($T = 30^\circ\text{C}$) at a throughput of 20 kg/h. Demineralized water was added with two 1.6 mm nozzles just before the first kneading zone, consisting of 8 pieces of 1/4 L/D kneading elements in a forward stagger angle of 60° . A second kneading zone, separated from the first kneading zone by a 1.5 L/D conveying element, was built up of 4 pieces of 1/4 L/D kneading elements in a forward stagger angle of 60° . Subsequently a conveying zone (3 L/D) was added and finally at the granulator outlet, 3 size control elements (1 L/D each) were included to reduce the oversized fraction. The unequal distribution of the kneading elements was based on previous research which concluded that more kneading elements in the first kneading zone yielded slightly better granule characteristics (less fines, lower friability, higher density and better flowability) (Portier et al., 2020b). Size control elements were added as these generate a narrower PSD (Portier et al., 2020c).

To avoid clogging of the dryer filters during granulator startup, the dryer was not connected during start-up of the granulator. After reaching steady state of the granulator, wet granules were transferred from the granulator outlet to the inlet of the segmented fluid bed dryer via vacuum transport. Steady state of the granulator was reached after 5–15 min and was assessed based on the stability of the barrel temperature at setpoint and the absence of torque drift. Each of the six segments was filled for 60 s, while maintaining an air flow of 340 m^3/h with an air temperature of 80°C . Granules were subsequently discharged to the product control hopper. To ensure a representative fill level at steady state conditions of the fluid bed dryer, the first five cells were discarded after reaching granulator steady state. As the relative drying time (i.e. drying time compared to fill time) was 5 at the upper drying time limit (Section 2.5), the fluid bed dryer only reached steady state after filling the fifth cell, when an equilibrium was reached between incoming wet granules and discharged dried granules. For each experiment, the granules from 6 cells were collected, generating a sample size of 2 kg (± 333 g/cell).

Table 1
Block scaling of variables in principal component analysis.

Block 1	Block 2	Block 3	Block 4	Block 5
Bulk density	d10	Span ratio	LOD	WBC
Tapped density	d50	d90-d10	Hygroscopicity	
	d90			

2.5. Design of experiments

Based on the PCA of the MCC batches (Section 3.1), four batches were selected and a two-level full factorial design was set up, including two center points. In each design identical process setting ranges were evaluated (Table 2). The included process variables were L/S ratio, screw speed and drying time. L/S ratio (0.24–0.27) was included as this is generally considered the most influential parameter in continuous twin screw wet granulation (El Hagrasy et al., 2013; Portier et al., 2020a, 2020b, 2020d; Thompson, 2015; Vercruyse et al., 2012). Furthermore, screw speed (500–800 rpm) was included as it can have an impact on the barrel fill level, shear and processability (Thompson, 2015). Finally, drying time (220–300 s) was included as the only variable of the dryer as this is one of the main driving factors to affect the residual moisture content (De Leersnyder et al., 2018). All ranges of the included process variables in the design of experiments, as well as constant factors such as throughput, dryer fill time, dryer air temperature and dryer air flow were based on preliminary tests in which all selected MCC batches were included.

To investigate the impact of MCC batch-to-batch variability together with the process parameters, the four full factorial designs were also evaluated in an integrated design of experiments, following a similar approach as Willecke et al. and Stauffer et al. (Stauffer et al., 2019a; Willecke et al., 2018). The impact of raw material attributes was evaluated through inclusion of the t1 and t2 scores of the PCA analysis (Table 2) in the integrated design of experiments.

MODDE pro (v 12.0, Sartorius Stedim Biotech, Malmö, Sweden) was used for setting up the design and analyzing the data. For each response, an interaction model was created using multiple linear regression (MLR). Models terms were hereby sequentially removed to optimize the predictive power (Q^2) of the corresponding model for each response. This process was iterated as long as the reduction of Q^2 was lower than 0.1 compared to highest achievable Q^2 . A main effect was only considered for removal if there was no significant contribution of its interactions. Sweet spot plots were constructed as an overlay of the individual MLR models. The sweet spot was defined as the area where the responses of interest were within the specified ranges (Section 3.5) (Eriksson et al., 2001).

2.6. Granule characterization

2.6.1. Loss on drying

The residual moisture content of the granules discharged from the fluid bed dryer was determined as described in Section 2.2.1.

2.6.2. Particle size distribution

Using a QICPIC particle size analyzer (Sympatec, Clausthal-Zellerfeld, Germany), the particle size distribution (PSD) of the granules (± 100 ml samples) was evaluated ($n = 3$). Granules were fed using a vibrating feeder and subsequently dispersed using a dry dispersion unit. The equivalent projected circle (EQPC) diameter was calculated for each particle using dynamic image analysis. The oversized and fine fraction were defined as particles $>1000 \mu\text{m}$ and $<150 \mu\text{m}$, respectively. Process yield was defined as the intermediate granular fraction, composed of granules with sizes between $150 \mu\text{m}$ and $1000 \mu\text{m}$. Based on the volumetric particle size distribution, the mass median diameter (d_{50}) was calculated.

2.6.3. Density and flowability

Granule flowability was derived from the Hausner ratio (HR), i.e. the ratio between tapped and bulk density (Eq. (1)), which were determined in triplicate (as described in Section 2.2.3).

$$HR = \frac{\rho_T}{\rho_B} \quad (1)$$

Table 2

Experimental design. QbD = Quality-by-Design batch; Com = Commercial batch.

L/S ratio	Screw speed (rpm)	Drying time (s)	MCC batch											
			QbD6			Com2			QbD1			QbD2		
			Exp N°	t1 score	t2 score	Exp N°	t1 score	t2 score	Exp N°	t1 score	t2 score	Exp N°	t1 score	t2 score
0.240	500	220	1	-1.45	1.28	11	2.47	1.32	21	-2.73	-0.27	31	0.61	-1.74
0.270	500	220	2	-1.45	1.28	12	2.47	1.32	22	-2.73	-0.27	32	0.61	-1.74
0.240	800	220	3	-1.45	1.28	13	2.47	1.32	23	-2.73	-0.27	33	0.61	-1.74
0.270	800	220	4	-1.45	1.28	14	2.47	1.32	24	-2.73	-0.27	34	0.61	-1.74
0.240	500	300	5	-1.45	1.28	15	2.47	1.32	25	-2.73	-0.27	35	0.61	-1.74
0.270	500	300	6	-1.45	1.28	16	2.47	1.32	26	-2.73	-0.27	36	0.61	-1.74
0.240	800	300	7	-1.45	1.28	17	2.47	1.32	27	-2.73	-0.27	37	0.61	-1.74
0.270	800	300	8	-1.45	1.28	18	2.47	1.32	28	-2.73	-0.27	38	0.61	-1.74
0.255	650	260	9	-1.45	1.28	19	2.47	1.32	29	-2.73	-0.27	39	0.61	-1.74
0.255	650	260	10	-1.45	1.28	20	2.47	1.32	30	-2.73	-0.27	40	0.61	-1.74

2.6.4. Friability

Friability was determined in triplicate using a friabilator (Pharmatest PTF E, Hainburg, Germany) equipped with a plexiglass abrasion drum with baffles. For each measurement 10 g (m_1) of a granular fraction >250 μm was added to the drum alongside 200 glass beads (4 mm, Carl Roth GmbH, Karlsruhe, Germany). After 250 revolutions (25 rpm), the glass beads were removed and the granular mass > 250 μm (m_2) was weighed. Granule friability was evaluated using Eq. (2). A 30% upper limit is hereby commonly used to indicate the boundary above which granules are prone to attrition and breakage during downstream processing.

$$Fr (\%) = \frac{m_1 - m_2}{m_1} \times 100 \quad (2)$$

2.7. Torque measurements

Torque values were measured at 1-s intervals using a built-in torque gauge. Only measurements acquired during filling of the fluid bed dryer at steady state conditions (Section 2.4), were used to calculate the average torque.

3. Results and discussion

3.1. MCC characterization and batch selection

The loading scatter plot of the PCA analysis (Fig. 1) illustrates that

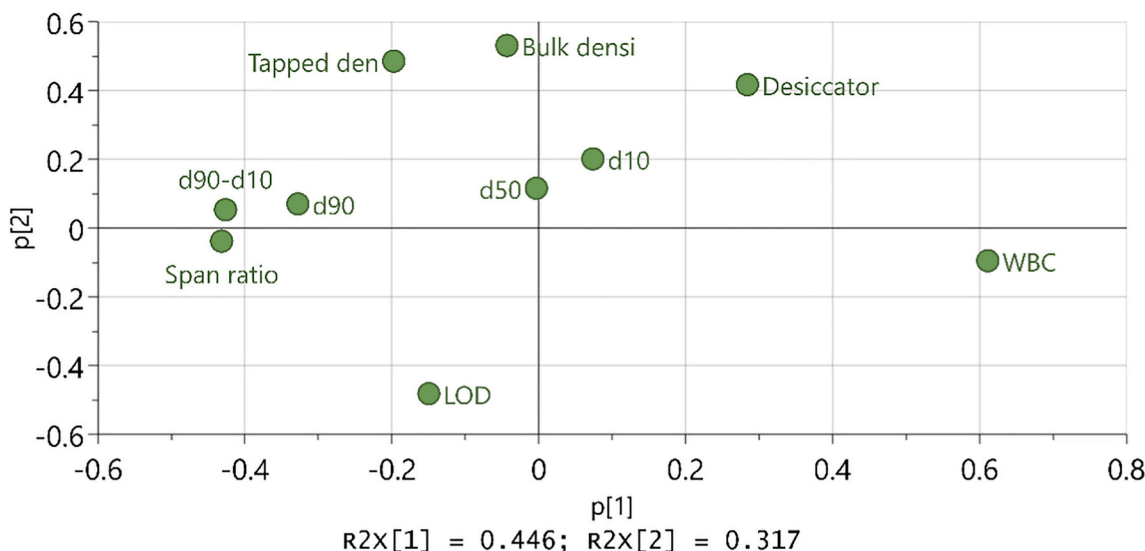


Fig. 1. Loading scatter plot of principle component analysis.

the variability of the first principal component (PC) was mostly dominated by the water binding capacity and differences in the width of the PSD. D90 was situated relatively close to the PSD width cluster whereas d10 and d50 were situated closer to the origin. This was explained by the calculation method of the PSD width metrics, which are mostly affected by d90 due to the limited absolute differences within d10 and d50 values (Table 3). The second PC was mostly impacted by density-related measures, hygroscopicity (desiccator) and moisture content (LOD). The two latter characteristics were clearly anticorrelated, as samples with higher LOD values, (indicating a higher amount of water already present in the powder bed), were less hygroscopic. In addition, an anticorrelation between bulk density and LOD was observed, which was attributed to enhanced inter-particulate friction at higher moisture content, resulting in a lower density. This phenomenon was previously described by Nicolas et al. for Avicel PH 302 (Nicolas et al., 1999).

The score scatter plot (Fig. 2), representing the variability between MCC batches, indicates that QbD batches were mostly situated in the left half of the scatter plot. This was also reflected in the average material characteristics for commercial versus QbD samples (Table 3). On average, QbD batches were characterized by a lower WBC and larger PSD width, accounting for the location at the left side of the scatter plot. Furthermore, QbD batches had a slightly higher LOD and lower degree of hygroscopicity. Consequently, they exhibited slightly more negative scores along PC2 than the commercial batches. In general, a similar degree of raw material variability was observed by Fonteyne et al., although broader PSD values were reported, potentially due to a

Table 3
Overview of raw data included in principal component analysis.

Batch	Bulk density (g/ml)	Tapped density (g/ml)	WBC (%)	LOD (%)	d10 (µm)	d50 (µm)	d90 (µm)	Span ratio	d90-d10 (µm)	Hygroscopicity (%)
Com1	0.34	0.46	185.0	4.37	20.12	57.43	130.45	1.92	110.33	3.84
Com2	0.35	0.45	195.2	4.39	20.61	55.35	108.01	1.58	87.40	4.50
Com3	0.35	0.46	190.7	4.29	21.23	57.89	119.85	1.70	98.62	4.38
Com4	0.33	0.44	196.6	5.14	21.04	58.33	120.77	1.71	99.72	3.54
Com5	0.31	0.42	189.9	5.61	19.36	54.50	113.03	1.72	93.67	3.15
Com6	0.34	0.45	195.3	5.27	18.49	54.66	113.41	1.74	94.92	3.91
QbD1	0.34	0.46	166.3	5.75	19.75	57.07	133.70	2.00	113.95	2.60
QbD2	0.32	0.43	192.5	5.67	19.65	56.13	118.91	1.77	99.26	3.03
QbD3	0.34	0.45	174.3	5.33	20.72	59.81	129.08	1.81	108.36	3.34
QbD4	0.33	0.44	177.7	5.37	20.45	57.22	125.74	1.84	105.29	3.23
QbD5	0.33	0.45	171.4	5.06	17.51	49.64	118.09	2.03	100.58	3.50
QbD6	0.35	0.46	162.8	4.77	20.09	55.11	124.74	1.90	104.65	3.83
Average commercial	0.34	0.45	192.1	4.85	20.14	56.36	117.59	1.73	97.44	3.89
Average Quality-by-Design	0.34	0.45	174.2	5.33	19.70	55.83	125.04	1.89	105.35	3.25

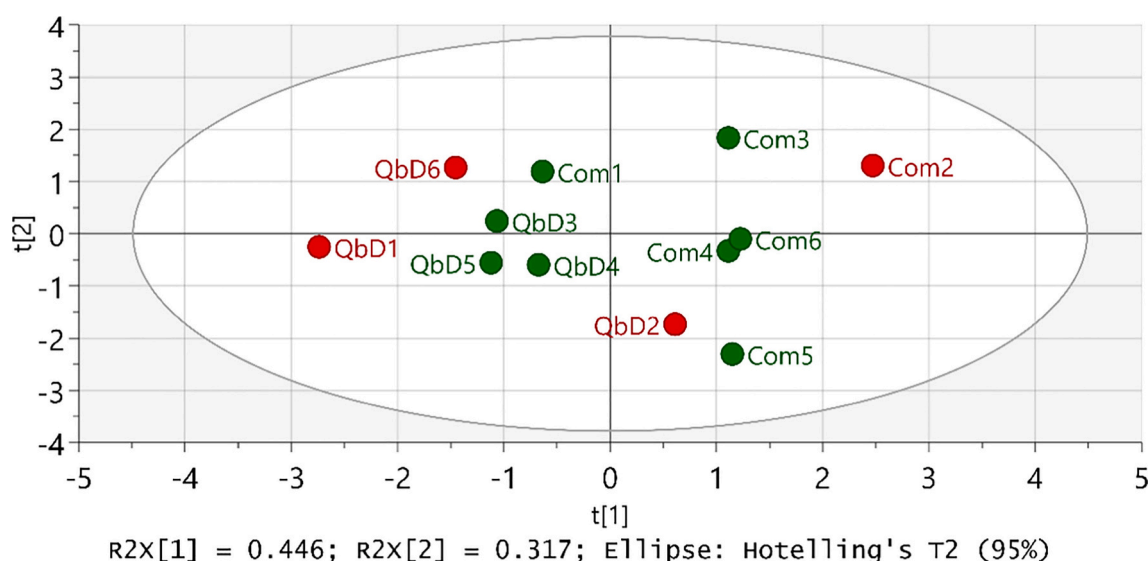


Fig. 2. Score scatter plot of principle component analysis. Selected MCC grades (1 in each quadrant) were indicated in red. (For interpretation of the references to colour in this figure legend, the reader is referred to the web version of this article.)

different way of measuring (dispersed in miglyol instead of dry dispersion) (Fonteyne et al., 2015). To capture a maximum of raw material variability in the subsequent design of experiments, the most extreme batch of each quadrant was selected (indicated in red in Fig. 2). However, the QbD2 batch was selected instead of the Com5 batch to represent the bottom right quadrant due to limited availability of Com5.

3.2. DoE model quality

For all responses, highly reproducible (> 0.5) MLR models with a good model fit ($R^2 > 0.5$) and predictive power ($Q^2 > 0.5$) were obtained, as illustrated in Fig. 3. R^2 is the model fit and indicates how much of the response variability is captured by the MLR model. Q^2 is an estimate of the predictive ability, based on internal cross-validation. The

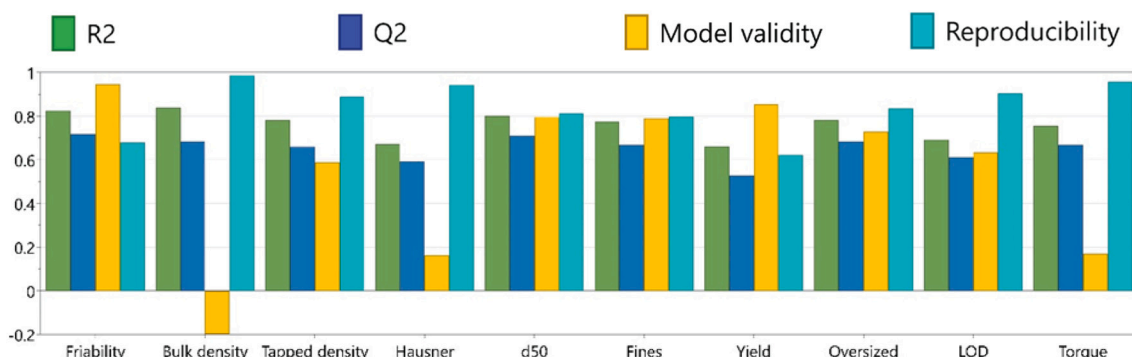


Fig. 3. Summary of fit plot.

poor model validity for bulk density, Hausner ratio and torque was attributed to their high reproducibility. As model validity is an estimate which compares the model uncertainty to the experimental error, poor model validity was obtained for these responses. Due to the relative nature of this estimate and the high Q^2 , R^2 and reproducibility, these models were considered suitable for use (Eriksson et al., 2001).

3.3. Granule characterization

3.3.1. Particle size distribution

Particle size-related measures, such as d50, the oversized, fine and yield fractions, were mainly affected by L/S ratio and raw material attributes (Fig. 4). The large impact of L/S ratio is inherent to this manufacturing technique and has been thoroughly investigated in several research papers (El Hagrasy et al., 2013; Fonteyne et al., 2015; Keleb et al., 2004; Portier et al., 2020c, 2020d, 2020a, 2020b; Vandevivere et al., 2019). Higher L/S ratios generated larger particles, which was mainly attributed to increased dissolution/wetting of lactose and metformin.HCl and improved binder activity. The small effect on the yield fraction is due to the intermediate nature of this response. As L/S ratio had opposite effects of similar magnitude on the fine and oversized fraction, the net effect on yield was indeed expected to be small. Overall, relatively high d50 values were obtained with all MCC batches, which is representative to how commercial formulations are generally processed. The general aim is to obtain a limited amount of fines after the dryer as fines are detrimental towards downstream processing (e.g. during tableting). The desired PSD can subsequently be reached in the milling unit, situated immediately after the dryer.

Raw material attributes (represented by t1 and t2 scores) had a significant impact on granule size (Table 4). A high t1 score, associated with high water binding capacity and narrow PSD, was detrimental towards granule formation (d50). A similar effect of water binding capacity was observed by Fonteyne et al. (Fonteyne et al., 2015). As MCC batches with a higher water binding capacity reduce the available amount of water for granulation, these batches are indeed expected to generate smaller granules. In contrast to the t1 score, a high t2 score, associated with high bulk density and low LOD, was favorable for granulation. Similarly, a study by Koo and Heng demonstrated that MCC with a higher bulk density required less water to produce spheronized particles of a specific particle size. Due to the more efficient packing of higher density particles, it was hypothesized that the smaller intra-particle voids (measured with mercury intrusion porosimetry)

Table 4

Average response value for PSD-related measures, grouped per MCC batch.

MCC batch	d50 (μm)	Fines (%)	Yield (%)	Oversized (%)
QbD1	1089	7.02	41.31	51.67
QbD2	755	15.30	43.85	40.85
QbD6	1047	7.83	41.68	50.49
Com2	924	11.00	42.07	46.93

accommodated less water, leaving more water available for particle growth at the particle surface (Koo and Heng, 2001). It was therefore concluded in current study that batches with a low WBC, low moisture content and high bulk density are preferred for continuous twin screw granulation.

The effect of screw speed was generally less pronounced but was still influential for most PSD-related measures. High screw speeds reduced the oversized fraction and d50 by reducing the barrel fill level and densification throughout the barrel (Dhenge et al., 2010; Thompson, 2015). No effect of the drying time was observed, indicating that particles inside the segmented fluid bed dryer were not prone to more attrition and breakage at increased drying times.

3.3.2. Bulk and tapped density

Despite limited differences in bulk (0.32–0.35 g/ml) and tapped density (0.43–0.46 g/ml) of the selected MCC batches, significantly larger differences were observed in the bulk (0.52–0.66 g/ml) and tapped density (0.68–0.80 g/ml) of the corresponding granules (Supplement 1). The largest effects were related to raw material attributes, similarly to particle size-related metrics (Fig. 5). Again, a low t1 score and a high t2 score were most favorable towards achieving granules with better quality attributes (limited amount of fines, low friability, free flowing granules). Due to the higher excipient density (t2), a more efficient intra-granular particle packing was observed, resulting in a higher granular density. As granules produced with MCC with a low WBC (low t1) have more water available for granulation, more densification occurred. Additionally, blends with a slightly broader particle size distribution (low t1) were more suited to fill up inter-particle voids, again increasing granular bulk and tapped density (Desmond and Weeks, 2014). In contrast, Fonteyne et al. reported no differences in granule density (Fonteyne et al., 2015), potentially caused by a different formulation or design setup. A limited detrimental effect was seen for high screw speeds, which was related to the lower barrel fill level. Drying time proved non-influential towards changes in granule bulk and

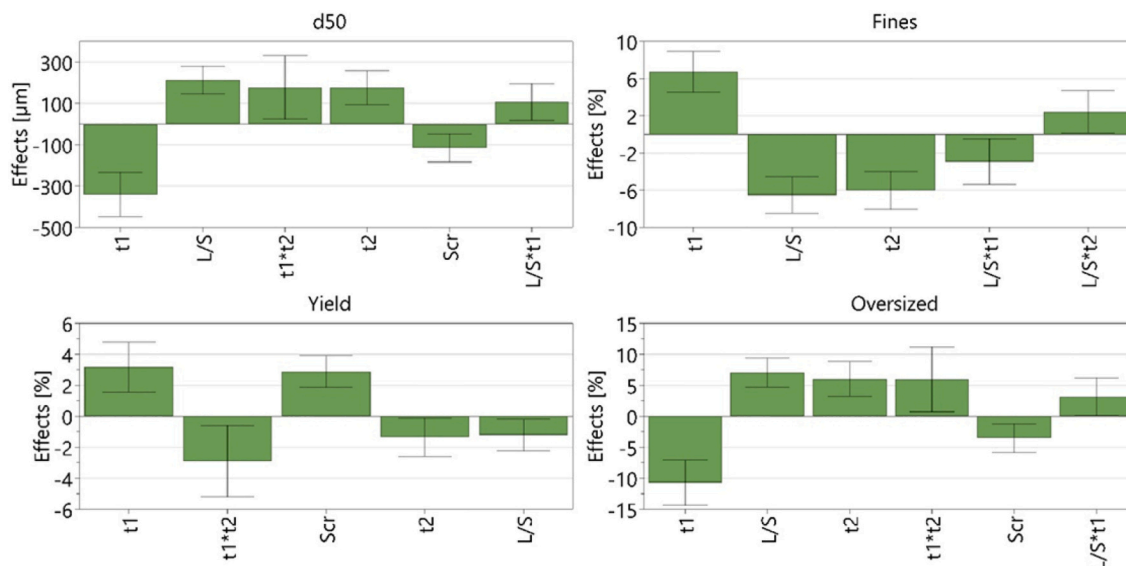


Fig. 4. Effect plots of particle size - related measures.

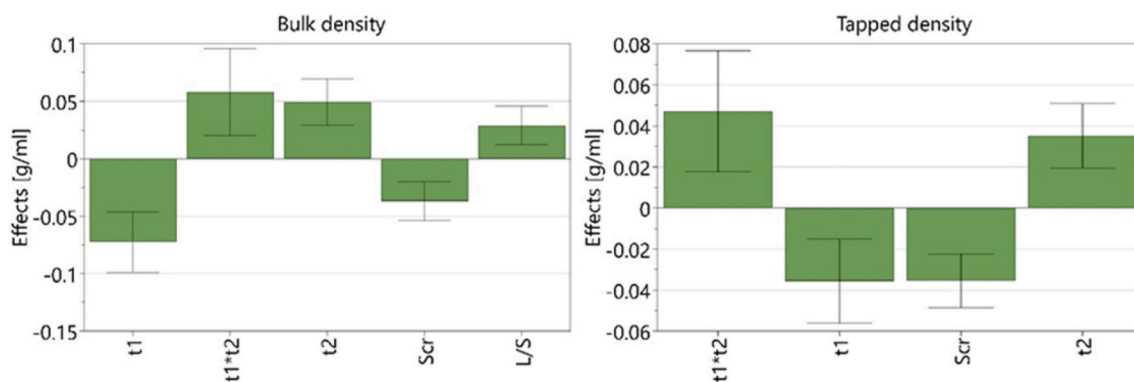


Fig. 5. Effect plots of bulk and tapped density.

tapped density.

3.3.3. Flowability

Most granules exhibited good or fair flow, according to the European Pharmacopoeia (European Directorate for the Quality of Medicine, 2017). However, for the QbD2 batch (Experiments 31–40), situated in the bottom right quadrant of the PCA plot, substantially worse flow properties were obtained (Fig. 6), which correlated with the observed lower granular density and smaller particle size. Although this was not a commercially available batch, the impact of raw material variability should not be neglected as the PCA plot indicated that commercial batches (Com5) are available with similar properties. Apart from the detrimental effect of t1 and favorable effect of t2, L/S ratio positively affected granule flow properties. No effect of screw speed or drying time was observed.

3.3.4. Friability

As shown in Fig. 7, granule friability was low for all experimental runs. Despite the low friability, it was clear that granules produced with the QbD2 batch (high t1, low t2) were more prone to attrition than granules produced with other MCC batches. This was also observed in the effects: raw material attributes associated with high t1 scores generated weaker granules whereas MCC characteristics leading to high t2 scores generated stronger granules. As t1 scores were mainly driven by WBC, high WBC proved detrimental towards granule strength. MCC particles with a lower WBC leave more water available for interaction with the binder and the water soluble filler (lactose), which contributes to granule strength. In addition, higher L/S ratios were favorable to reduce granule friability, similar to previous research (Portier et al., 2020b, 2020a).

3.3.5. Loss on drying

The residual moisture content of granules discharged from the semi-continuous fluid bed dryer varied between 1.73 and 5.39% (Supplement 1). The LOD was solely influenced by the drying time and L/S ratio, which had an effect of -1.40% and +1.22%, respectively. These results were in line with expectations as longer drying times lead to higher drying capacity and lower granular moisture contents. Despite the clear effect on other granule characteristics, raw material attributes did not impact LOD, indicating that the resulting granule size and density differences did not impact the drying process for this formulation.

3.4. Torque measurements

Average torque values varied over a wide range, from 1.5 to 15.5 Nm. Although relatively high torque values are typical when processing MCC via twin screw granulation (Portier et al., 2020c, 2020a), the impact of the MCC raw material properties was remarkably high. As a high t2 score and a low t1 score generated larger and denser particles, it was indeed expected that such scores increase the average torque (Fig. 8), in accordance with previous studies on similar formulations (Portier et al., 2020a; Portier et al., 2020c). These larger and denser particles are associated with high frictional forces and a high fill level in the granulator kneading zones, hence generating high torque values. As the continuous granulator stops when exceeding the safety limit (20 Nm for this setup), the impact of raw material variability should be controlled during manufacturing in order to ensure the robustness of manufacturability. The relevance of the process-related factors was in line with previous studies as a higher screw speed reduced torque, whereas a high water content generated increased torque averages (Dhenge et al., 2012; Portier et al., 2020c; Vanhoorne et al., 2016b, 2016a).

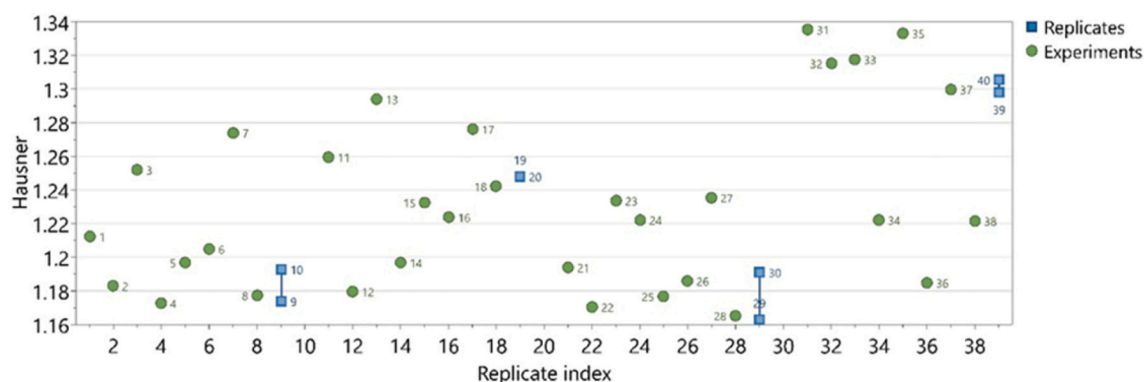


Fig. 6. Replicate plot of Hausner ratio.

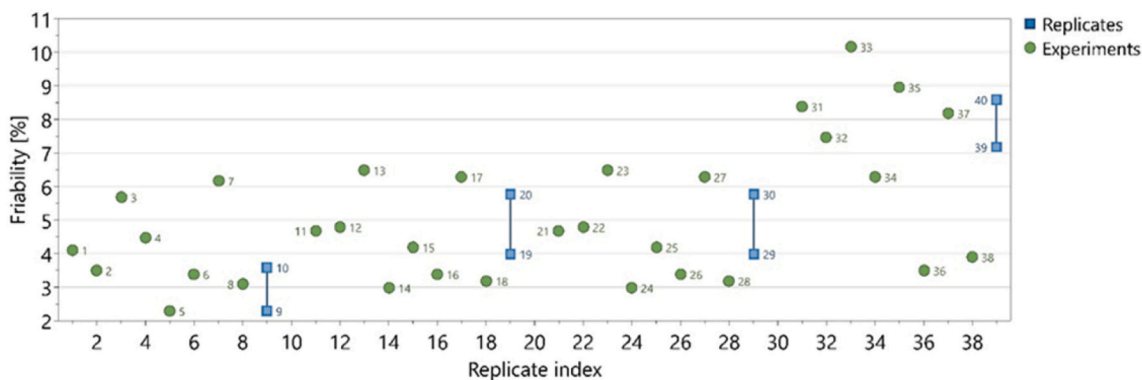


Fig. 7. Replicate plot of friability.

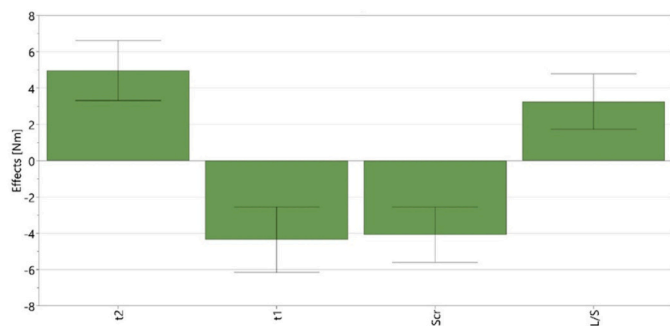


Fig. 8. Effect plot of average torque.

3.5. Applicability of integrated QbD approaches in pharmaceutical manufacturing

Currently many manufacturing optimization efforts in continuous manufacturing are classified as QbD but are still limited to technical process understanding, not taking into account the raw material attributes affecting the critical quality attributes (Baronsky-Probst et al.,

2016; Maniruzzaman et al., 2017). Hence a fundamental understanding is lacking on how to ensure that the process consistently delivers drug product complying with the quality target product profile, which is essential for a holistic QbD approach (Grangeia et al., 2020; Politis et al., 2017; Yu et al., 2014). The approach used in current study offers a hybrid approach, integrating both process settings and critical material attributes in a quantitative way, in accordance with the recent FDA guidance on quality considerations for continuous manufacturing (U.S. Food and Drug Administration, 2019). As illustrated in the sweet spot plot (Fig. 9), the manufacturing process for the studied formulation could be adapted in most cases to accommodate changes in raw material variability. In this example, four constraints were used (fines <10%, Hausner ratio < 1.25, torque <10 Nm and LOD between 1 and 3%) to illustrate the trade-off between processability and reaching desirable granule characteristics. To limit the amount of fines and improve flow properties, higher L/S ratios are favorable, although these also increase torque and residual moisture content.

Models could be continuously adapted based on novel insights towards critical material attributes as well as data generated during future production. Consequently, this concept is perfectly suited for integration in drug product enhancement. Apart from MCC, this approach can also be expanded to other excipients (fillers, binders, disintegrants,

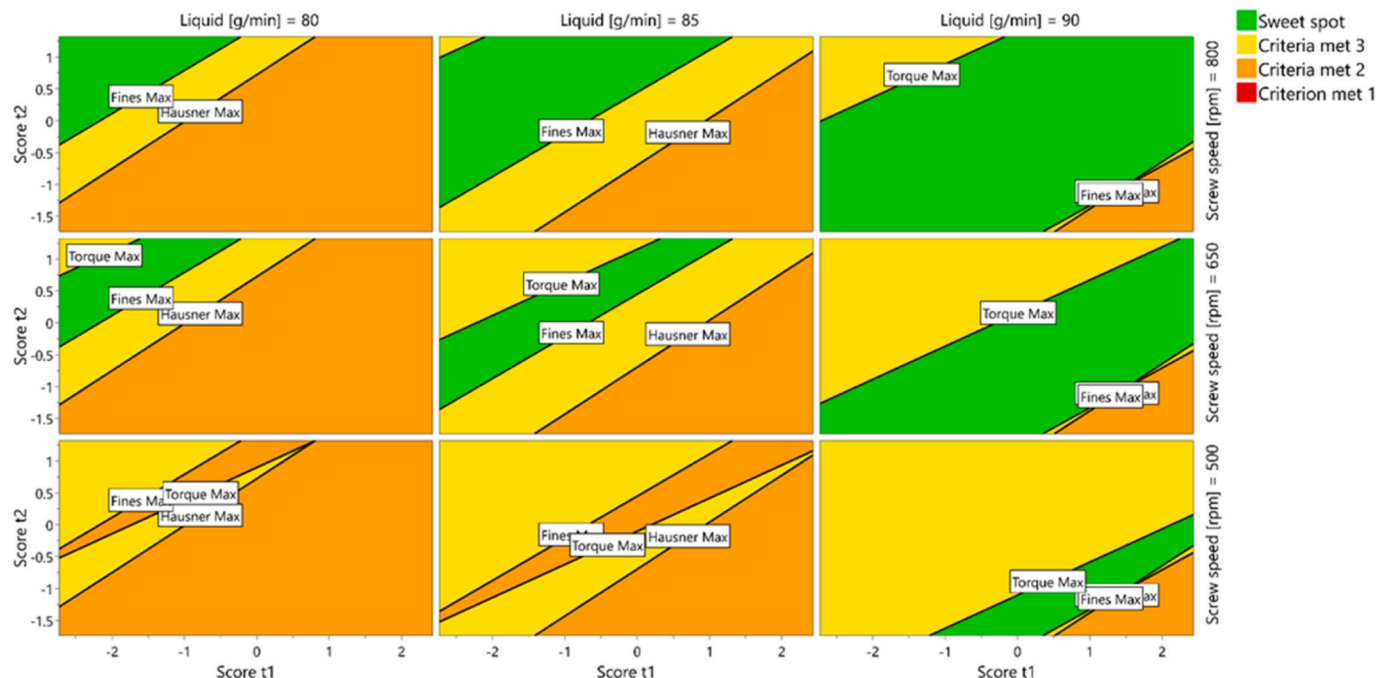


Fig. 9. Sweet spot plot including criteria: fines <10%, Hausner ratio < 1.25, torque <10 Nm and LOD between 1 and 3%.

lubricants ...) and APIs. For each of these compounds a different subset of critical material attributes can be included, based on raw material batch-to-batch variability as well as process understanding. Several risk management strategies could be developed, based on these data-driven models.

A first risk management strategy could be based on the raw material attributes and subsequent process understanding to steer the individual unit operations of a continuous manufacturing line, hence ensuring high quality and reproducibility of the drug product. To ensure a proper control strategy, knowledge on residence time distribution (RTD) of material throughout a manufacturing line is critical. In recent years, several studies have been published on RTD of individual unit operations such as feeding (Toson and Khinast, 2019; Van Snick et al., 2019), blending (Karttunen et al., 2019; Van Snick et al., 2017), granulation (Kumar et al., 2016; Li et al., 2014; Meier et al., 2017) and tableting (De Leersnyder et al., 2019; Dülle et al., 2019; Puckhaber et al., 2020), indicating the rapidly increasing interest in this field. This approach would be most favorable for novel drug product development where limited data is available and for manufacturing drug products which have a limited design space.

Alternatively, a more conservative approach could be implemented in which process settings are not adaptable, but constraints are put on the acceptable raw material properties. Based on the insights on the interplay between process parameters and raw material attributes, quantitative constraints such as API particle shape, excipient flowability and hygroscopicity can be derived to ensure reaching the quality target product profile. Although this approach requires significantly less resources (residence time distribution data, control loops, system integration), the potential gain during manufacturing is significantly lower as there is no active control during manufacturing. Therefore, this approach could be more suitable for well-established manufacturing processes which are less susceptible to raw material variability.

4. Conclusion

In this study, the impact of MCC raw material variability and process settings towards processing in a continuous wet granulation and semi-continuous drying line was assessed. Based on principal component analysis, variability in raw material characteristics (indicated by t1 and t2 scores) was evaluated. Compared to screw speed and drying time, L/S ratio had a larger effect on granule quality attributes and processability. A similar to larger impact of the t1 and t2 scores was found, indicating the importance of raw material attributes. A clear correlation between these characteristics and granule quality attributes was found, which highlights the risk of batch-to-batch excipient variability affecting downstream processes such as tableting.

As a higher t1 score was associated with smaller granules, poorer flow properties, higher friability and lower density, it was apparent that this score should be minimized in order to obtain granules with the required critical quality attributes (CQAs). The t1 score was mainly dominated by the water binding capacity and the width of the particle size distribution, between which no causal relationship was established. MCC batches with lower WBC exhibited more residual water available for granule growth within the barrel, partially accounted for by higher dissolution of the water soluble components in the selected model formulation. In contrast to the t1 score, a higher t2 score was beneficial towards granule CQAs. As this principal component was driven by bulk density and LOD, situated on opposite sides of the loading plot, MCC batches with a high bulk density and low LOD should be preferred for commercial production. It was therefore concluded that MCC batches with a low water binding capacity, low moisture content and high bulk density resulted in granules with better quality.

The integrated approach described above can also be expanded to other excipients as well as active pharmaceutical ingredients (APIs), opening the path towards flexible manufacturing to assure consistent drug product quality. Furthermore, additional excipient or API

characteristics could be added or removed to optimize the models.

Declaration of Competing Interest

The authors declare that they have no known competing financial interests or personal relationships that could have appeared to influence the work reported in this paper.

Acknowledgments

This work was supported by Janssen Pharmaceutica and the agency Flanders Innovation and Entrepreneurship (IWT project n° 145059). DuPont is acknowledged for kindly providing the MCC batches.

Appendix A. Supplementary data

Supplementary data to this article can be found online at <https://doi.org/10.1016/j.ijph.2021.100077>.

References

- Baronsky-Probst, J., Möltgen, C.V., Kessler, W., Kessler, R.W., 2016. Process design and control of a twin screw hot melt extrusion for continuous pharmaceutical tamper-resistant tablet production. *Eur. J. Pharm. Sci.* 87, 14–21. <https://doi.org/10.1016/j.ejps.2015.09.010>.
- Byrn, S., Futran, M., Thomas, H., Jayjock, E., Maron, N., Meyer, R.F., Myerson, A.S., Thien, M.P., Trout, B.L., 2015. Achieving continuous manufacturing for final dosage formation: challenges and how to meet them May 20-21, 2014 continuous manufacturing symposium. *J. Pharm. Sci.* <https://doi.org/10.1002/jps.24247>.
- De Leersnyder, F., Vanhoorne, V., Bekaert, H., Verduyck, J., Ghijs, M., Bostijn, N., Verstraeten, M., Cappuyns, P., Van Assche, I., Vander Heyden, Y., Ziemons, E., Remon, J.P., Nopens, I., Vervaet, C., De Beer, T., 2018. Breakage and drying behaviour of granules in a continuous fluid bed dryer: influence of process parameters and wet granule transfer. *Eur. J. Pharm. Sci.* 115, 223–232. <https://doi.org/10.1016/j.ejps.2018.01.037>.
- De Leersnyder, F., Vanhoorne, V., Kumar, A., Vervaet, C., De Beer, T., 2019. Evaluation of an in-line NIR spectroscopic method for the determination of the residence time in a tablet press. *Int. J. Pharm.* 565, 358–366. <https://doi.org/10.1016/j.ijpharm.2019.05.006>.
- Desmond, K.W., Weeks, E.R., 2014. Influence of particle size distribution on random close packing of spheres. *Phys. Rev. E - Stat. Nonlinear, Soft Matter Phys.* 90 <https://doi.org/10.1103/PhysRevE.90.022204>.
- Dhenge, R.M., Fyles, R.S., Cartwright, J.J., Doughty, D.G., Hounslow, M.J., Salman, A.D., 2010. Twin screw wet granulation: granule properties. *Chem. Eng. J.* 164, 322–329. <https://doi.org/10.1016/j.cej.2010.05.023>.
- Dhenge, R.M., Cartwright, J.J., Hounslow, M.J., Salman, A.D., 2012. Twin screw wet granulation: effects of properties of granulation liquid. *Powder Technol.* 229, 126–136. <https://doi.org/10.1016/j.powtec.2012.06.019>.
- Djuric, D., Kleinebudde, P., 2008. Impact of screw elements on continuous granulation with a twin-screw extruder. *J. Pharm. Sci.* 97, 4934–4942. <https://doi.org/10.1002/jps.21339>.
- Dülle, M., Özcan, H., Leopold, C.S., 2019. Influence of the feed frame design on the powder behavior and the residence time distribution. *Int. J. Pharm.* 565, 523–532. <https://doi.org/10.1016/j.ijpharm.2019.05.026>.
- El Hagrasy, A.S., Hennenkamp, J.R., Burke, M.D., Cartwright, J.J., Litster, J.D., 2013. Twin screw wet granulation: Influence of formulation parameters on granule properties and growth behavior. *Powder Technol.* 238, 108–115. <https://doi.org/10.1016/j.powtec.2012.04.035>.
- Eriksson, L., Johansson, E., Wold, N.K., Wikström, C., Wold, S., 2001. Design of Experiments, Principles and Applications, Third. ed. *Journal of Chemometrics, MKS Umetrics AB*. <https://doi.org/10.1002/cem.686>.
- European Directorate for the Quality of Medicine, 2017. *European Pharmacopoeia 9.0: 2.9.36 Powder Flow*.
- Fonteyne, M., Wickström, H., Peeters, E., Verduyck, J., Ehlers, H., Peters, B.H., Remon, J.P., Vervaet, C., Ketolainen, J., Sandler, N., Rantanen, J., Naelapää, K., De Beer, T., 2014. Influence of raw material properties upon critical quality attributes of continuously produced granules and tablets. *Eur. J. Pharm. Biopharm.* 87, 252–263. <https://doi.org/10.1016/j.ejpb.2014.02.011>.
- Fonteyne, M., Correia, A., De Plecker, S., Verduyck, J., Ilić, I., Zhou, Q., Vervaet, C., Remon, J.P., Onofre, F., Bulone, V., De Beer, T., 2015. Impact of microcrystalline cellulose material attributes: a case study on continuous twin screw granulation. *Int. J. Pharm.* 478, 705–717. <https://doi.org/10.1016/j.ijpharm.2014.11.070>.
- Grangeia, H.B., Silva, C., Simões, S.P., Reis, M.S., 2020. Quality by design in pharmaceutical manufacturing: a systematic review of current status, challenges and future perspectives. *Eur. J. Pharm. Biopharm.* 147, 19–37. <https://doi.org/10.1016/j.ejpb.2019.12.007>.
- Harting, J., Kleinebudde, P., 2018. Development of an in-line Raman spectroscopic method for continuous API quantification during twin-screw wet granulation. *Eur. J. Pharm. Biopharm.* 125, 169–181. <https://doi.org/10.1016/j.ejpb.2018.01.015>.

- Ito, A., Kleinebudde, P., 2019. Influence of granulation temperature on particle size distribution of granules in twin-screw granulation (TSG). *Pharm. Dev. Technol.* 24, 874–882. <https://doi.org/10.1080/10837450.2019.1615089>.
- Karttunen, A.P., Hörmann, T.R., De Leersnyder, F., Ketolainen, J., De Beer, T., Hsiao, W. K., Korhonen, O., 2019. Measurement of residence time distributions and material tracking on three continuous manufacturing lines. *Int. J. Pharm.* 563, 184–197. <https://doi.org/10.1016/j.ijpharm.2019.03.058>.
- Keleb, E.L., Vermeire, A., Vervae, C., Remon, J.P., 2004. Twin screw granulation as a simple and efficient tool for continuous wet granulation. *Int. J. Pharm.* 273, 183–194. <https://doi.org/10.1016/j.ijpharm.2004.01.001>.
- Koo, O.M.Y., Heng, P.W.S., 2001. The influence of microcrystalline cellulose grade on shape and shape distributions of pellets produced by extrusion-spheronization. *Chem. Pharm. Bull.* 49, 1383–1387. <https://doi.org/10.1248/cpb.49.1383>.
- Kumar, A., Alakarjula, M., Vanhoorne, V., Toiviainen, M., De Leersnyder, F., Vercruyse, J., Juuti, M., Ketolainen, J., Vervae, C., Remon, J.P., Gernaey, K.V., De Beer, T., Nopens, I., 2016. Linking granulation performance with residence time and granulation liquid distributions in twin-screw granulation: an experimental investigation. *Eur. J. Pharm. Sci.* 90, 25–37. <https://doi.org/10.1016/j.ejps.2015.12.021>.
- Li, H., Thompson, M.R., O'Donnell, K.P., 2014. Understanding wet granulation in the kneading block of twin screw extruders. *Chem. Eng. Sci.* 113, 11–21. <https://doi.org/10.1016/j.ces.2014.03.007>.
- Liu, H., Galbraith, S.C., Park, S.Y., Cha, B., Huang, Z., Meyer, R.F., Flamm, M.H., O'Connor, T., Lee, S., Yoon, S., 2019. Assessment of spatial heterogeneity in continuous twin screw wet granulation process using three-compartmental population balance model. *Pharm. Dev. Technol.* 24, 105–117. <https://doi.org/10.1080/10837450.2018.1427106>.
- Madarász, L., Nagy, Z.K., Hoffer, I., Szabó, Barnabás, Csontos, I., Patakai, H., Démuth, B., Szabó, Bence, Csorba, K., Marosi, G., 2018. Real-time feedback control of twin-screw wet granulation based on image analysis. *Int. J. Pharm.* 547, 360–367. <https://doi.org/10.1016/j.ijpharm.2018.06.003>.
- Maniruzzaman, M., Ross, S.A., Dey, T., Nair, A., Snowden, M.J., Douroumis, D., 2017. A quality by design (QbD) twin-screw extrusion wet granulation approach for processing water insoluble drugs. *Int. J. Pharm.* 526, 496–505. <https://doi.org/10.1016/j.ijpharm.2017.05.020>.
- Meier, R., Moll, K.P., Krumme, M., Kleinebudde, P., 2017. Impact of fill-level in twin-screw granulation on critical quality attributes of granules and tablets. *Eur. J. Pharm. Biopharm.* 115, 102–112. <https://doi.org/10.1016/j.ejpb.2017.02.010>.
- Nicolas, V., Chabain, O., André, C., Rochat-Gonthier, M.H., Pourcelot, Y., 1999. Preformulation: effect of moisture content on microcrystalline cellulose (Avicel PH-302) and its consequences on packing performances. *Drug Dev. Ind. Pharm.* 25, 1137–1142. <https://doi.org/10.1081/DDC-100102280>.
- Pauli, V., Roggo, Y., Kleinebudde, P., Krumme, M., 2019. Real-time monitoring of particle size distribution in a continuous granulation and drying process by near infrared spectroscopy. *Eur. J. Pharm. Biopharm.* 141, 90–99. <https://doi.org/10.1016/j.ejpb.2019.05.007>.
- Politis, S.N., Colombo, P., Colombo, G., Rekkas, D.M., 2017. Design of experiments (DoE) in pharmaceutical development. *Drug Dev. Ind. Pharm.* 43, 889–901. <https://doi.org/10.1080/03639045.2017.1291672>.
- Portier, C., De Vriendt, C., Vigh, T., Di Pretoro, G., De Beer, T., Vervae, C., Vanhoorne, V., 2020a. Continuous twin screw granulation: robustness of lactose/MCC-based formulations. *Int. J. Pharm.* 588, 119756. <https://doi.org/10.1016/j.ijpharm.2020.119756>.
- Portier, C., Pandelaere, K., Delaet, U., Vigh, T., Di Pretoro, G., De Beer, T., Vervae, C., Vanhoorne, V., 2020b. Continuous twin screw granulation: a complex interplay between formulation properties, process settings and screw design. *Int. J. Pharm.* 576, 119004. <https://doi.org/10.1016/j.ijpharm.2019.119004>.
- Portier, C., Pandelaere, K., Delaet, U., Vigh, T., Kumar, A., Di Pretoro, G., De Beer, T., Vervae, C., Vanhoorne, V., 2020c. Continuous twin screw granulation: influence of process and formulation variables on granule quality attributes of model formulations. *Int. J. Pharm.* 576, 118981. <https://doi.org/10.1016/j.ijpharm.2019.118981>.
- Portier, C., Vigh, T., Di Pretoro, G., De Beer, T., Vervae, C., Vanhoorne, V., 2020d. Continuous twin screw granulation: impact of binder addition method and surfactants on granulation of a high-dosed, poorly soluble API. *Int. J. Pharm.* 577, 119068. <https://doi.org/10.1016/j.ijpharm.2020.119068>.
- Puckhaber, D., Eichler, S., Kwade, A., Finke, J.H., 2020. Impact of particle and equipment properties on residence time distribution of pharmaceutical excipients in rotary tablet presses. *Pharmaceutics* 12, 283. <https://doi.org/10.3390/pharmaceutics12030283>.
- Shirazian, S., Ismail, H.Y., Singh, M., Shaikh, R., Croker, D.M., Walker, G.M., 2019. Multi-dimensional population balance modelling of pharmaceutical formulations for continuous twin-screw wet granulation: determination of liquid distribution. *Int. J. Pharm.* 566, 352–360. <https://doi.org/10.1016/j.ijpharm.2019.06.001>.
- Stauffer, F., Vanhoorne, V., Pilcer, G., Chavez, P.F., Vervae, C., De Beer, T., 2019a. Managing API raw material variability during continuous twin-screw wet granulation. *Int. J. Pharm.* 561, 265–273. <https://doi.org/10.1016/j.ijpharm.2019.03.012>.
- Stauffer, F., Vanhoorne, V., Pilcer, G., Chavez, P.F., Vervae, C., De Beer, T., 2019b. Managing API raw material variability in a continuous manufacturing line – Prediction of process robustness. *Int. J. Pharm.* 569, 118525. <https://doi.org/10.1016/j.ijpharm.2019.118525>.
- Thompson, M.R., 2015. Twin screw granulation-review of current progress. *Drug Dev. Ind. Pharm.* 41, 1223–1231. <https://doi.org/10.3109/03639045.2014.983931>.
- Thompson, M.R., Sun, J., 2010. Wet granulation in a twin-screw extruder: implications of screw design. *J. Pharm. Sci.* 99, 2090–2103. <https://doi.org/10.1002/jps.21973>.
- Toson, P., Khinast, J.G., 2019. Particle-level residence time data in a twin-screw feeder. *Data Br.* 27, 104672. <https://doi.org/10.1016/j.dib.2019.104672>.
- U.S. Food and Drug Administration, 2018. FDA approves lorlatinib for second- or third-line treatment of ALK-positive metastatic NSCLC [WWW Document]. *Case Med. Res.* <https://doi.org/10.31525/fda1-ucm625027.htm>.
- U.S. Food and Drug Administration, 2019. *Quality Considerations for Continuous Manufacturing - Guidance for Industry - Draft Guidance*.
- Van Snick, B., Holman, J., Vanhoorne, V., Kumar, A., De Beer, T., Remon, J.P., Vervae, C., 2017. Development of a continuous direct compression platform for low-dose drug products. *Int. J. Pharm.* 529, 329–346. <https://doi.org/10.1016/j.ijpharm.2017.07.003>.
- Van Snick, B., Kumar, A., Verstraeten, M., Pandelaere, K., Dhondt, J., Di Pretoro, G., De Beer, T., Vervae, C., Vanhoorne, V., 2019. Impact of material properties and process variables on the residence time distribution in twin screw feeding equipment. *Int. J. Pharm.* 556, 200–216. <https://doi.org/10.1016/j.ijpharm.2018.11.076>.
- Vandevivere, L., Portier, C., Vanhoorne, V., Hausler, O., Simon, D., De Beer, T., Vervae, C., 2019. Native starch as in situ binder for continuous twin screw wet granulation. *Int. J. Pharm.* 571, 118760. <https://doi.org/10.1016/j.ijpharm.2019.118760>.
- Vanhoorne, V., Janssens, L., Vercruyse, J., De Beer, T., Remon, J.P., Vervae, C., 2016a. Continuous twin screw granulation of controlled release formulations with various HPMC grades. *Int. J. Pharm.* 511, 1048–1057. <https://doi.org/10.1016/j.ijpharm.2016.08.020>.
- Vanhoorne, V., Vanbillemont, B., Vercruyse, J., De Leersnyder, F., Gomes, P., De Beer, T., Remon, J.P., Vervae, C., 2016b. Development of a controlled release formulation by continuous twin screw granulation: Influence of process and formulation parameters. *Int. J. Pharm.* 505, 61–68. <https://doi.org/10.1016/j.ijpharm.2016.03.058>.
- Vercruyse, J., Córdoba Díaz, D., Peeters, E., Fonteyne, M., Delaet, U., Van Assche, I., De Beer, T., Remon, J.P., Vervae, C., 2012. Continuous twin screw granulation: Influence of process variables on granule and tablet quality. *Eur. J. Pharm. Biopharm.* 82, 205–211. <https://doi.org/10.1016/j.ejpb.2012.05.010>.
- Vercruyse, J., Burggraef, A., Fonteyne, M., Cappuyens, P., Delaet, U., Van Assche, I., De Beer, T., Remon, J.P., Vervae, C., 2015. Impact of screw configuration on the particle size distribution of granules produced by twin screw granulation. *Int. J. Pharm.* 479, 171–180. <https://doi.org/10.1016/j.ijpharm.2014.12.071>.
- Verstraeten, M., Van Hauwermeiren, D., Hellings, M., Hermans, E., Geens, J., Vervae, C., Nopens, I., De Beer, T., 2018. Model-based NIR spectroscopy implementation for in-line assay monitoring during a pharmaceutical suspension manufacturing process. *Int. J. Pharm.* 546, 247–254. <https://doi.org/10.1016/j.ijpharm.2018.05.043>.
- Vervae, C., Remon, J.P., 2005. Continuous granulation in the pharmaceutical industry. *Chem. Eng. Sci.* 60, 3949–3957. <https://doi.org/10.1016/j.ces.2005.02.028>.
- Willecke, N., Szepes, A., Wunderlich, M., Remon, J.P., Vervae, C., De Beer, T., 2018. A novel approach to support formulation design on twin screw wet granulation technology: Understanding the impact of overarching excipient properties on drug product quality attributes. *Int. J. Pharm.* 545, 128–143. <https://doi.org/10.1016/j.ijpharm.2018.04.017>.
- Yu, L.X., 2016. Continuous Manufacturing Has a Strong Impact on Drug Quality [WWW Document]. U.S. Food Drug Adm, URL. <https://blogs.fda.gov/fdavoices/index.php/2016/04/continuous-manufacturing-has-a-strong-impact-on-drug-quality>.
- Yu, L.X., Amidon, G., Khan, M.A., Hoag, S.W., Polli, J., Raju, G.K., Woodcock, J., 2014. Understanding pharmaceutical quality by design. *AAAPS J.* 16, 771–783. <https://doi.org/10.1208/s12248-014-9598-3>.